individuals (Figure 1C,E**), representing an impaired induction after vaccination when normalised to an individual's day 0 baseline (**Figure 1F**). Together, these data indicate that the GC-Tfh cell response to vaccination is impaired in older persons.**

Tfh cell and GC responses are impaired in ageing

A major limitation of human vaccination studies is the difficulty of sampling secondary lymphoid

younger adult mice (Figure 2C**). This corresponded to a reduction in GC size (**Figure 2D**) and reduced levels of antigen-specific antibodies in the serum of aged mice (**Figure 2E–G**), consistent with previous reports that GC and antibody responses are reduced in magnitude in aged mice (**Kosco et al., 1989**; Szakal et al., 1990**; Yang et al., 1996**; van Dijk-Härd et al., 1997**; Eaton et al., 2004**; Linterman, 2014**). This deficiency in the GC response was coupled with reduced numbers of total CXCR5^{hi}PD-1^{hi}Foxp3^{-}CD4^{+} Tfh cells prior to, and ten days after immunisation, as well as significantly fewer antigen-specific Tfh cells, as assessed using 1W1K-loaded MHC-II tetramers (**Figure 2H–M**; gating strategy in **Figure 2—figure supplement 1**; key resources are listed in **Supplementary file 1**). This demonstrates that aged mice have impaired Tfh cell formation after immunisation, which recapitulates the age-associated defect in Tfh cell formation observed in humans (**Figure 1**).**

T cell priming is impaired in aged mice

The age-associated deficit in Tfh cells upon immunisation could be due to T cell-intrinsic changes with age, or due to the age of the microenvironment in which the T cells reside. After adoptive transfer of either TCR-transgenic TCR7 or OTII CD4 T cells from 2 to 3 month-old mice into young adult

surface of GFP$^+$ CD11b$^+$ cDC2s was also diminished, indicating impaired activation of cDC2s with age (

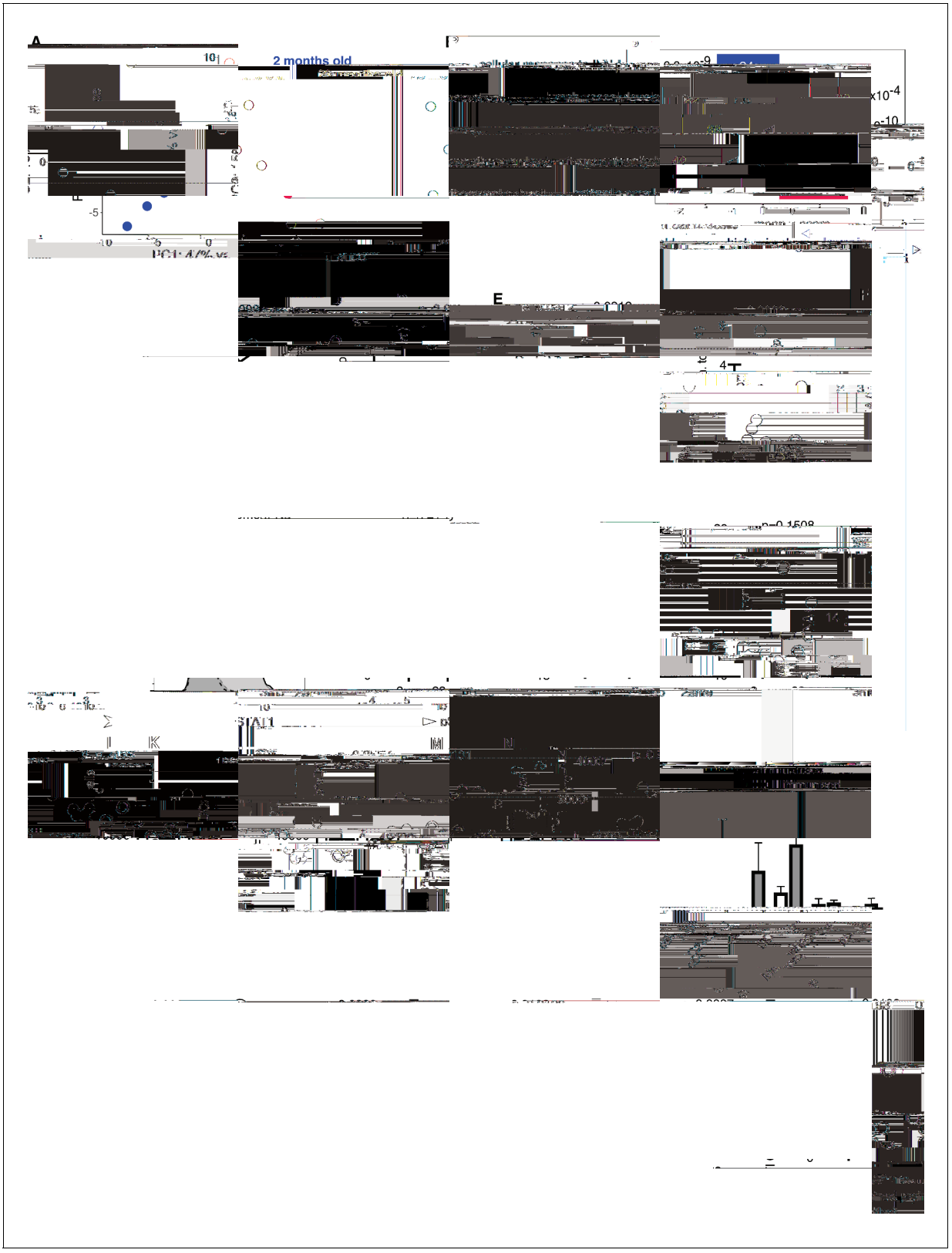

Figure 4. Reduced type I interferon (IFN-I) signalling in cDC2s from aged mice. (**A**) Principal component analysis (PCA) of the 1000 genes with the largest variance in sorted GFP^{+}CD11b

(

signature to another dataset (Franco et al., 2013**;** Nakaya et al., 2015**) showed that these genes were induced in older persons after influenza vaccination, but to a lesser extent than in younger people (**Figure 5B**), similar to our findings in aged mice (**Figure 4**). We performed PCA of the curated vaccine-induced IFN-I genes to determine how much an individual's IFN-I gene signature had**

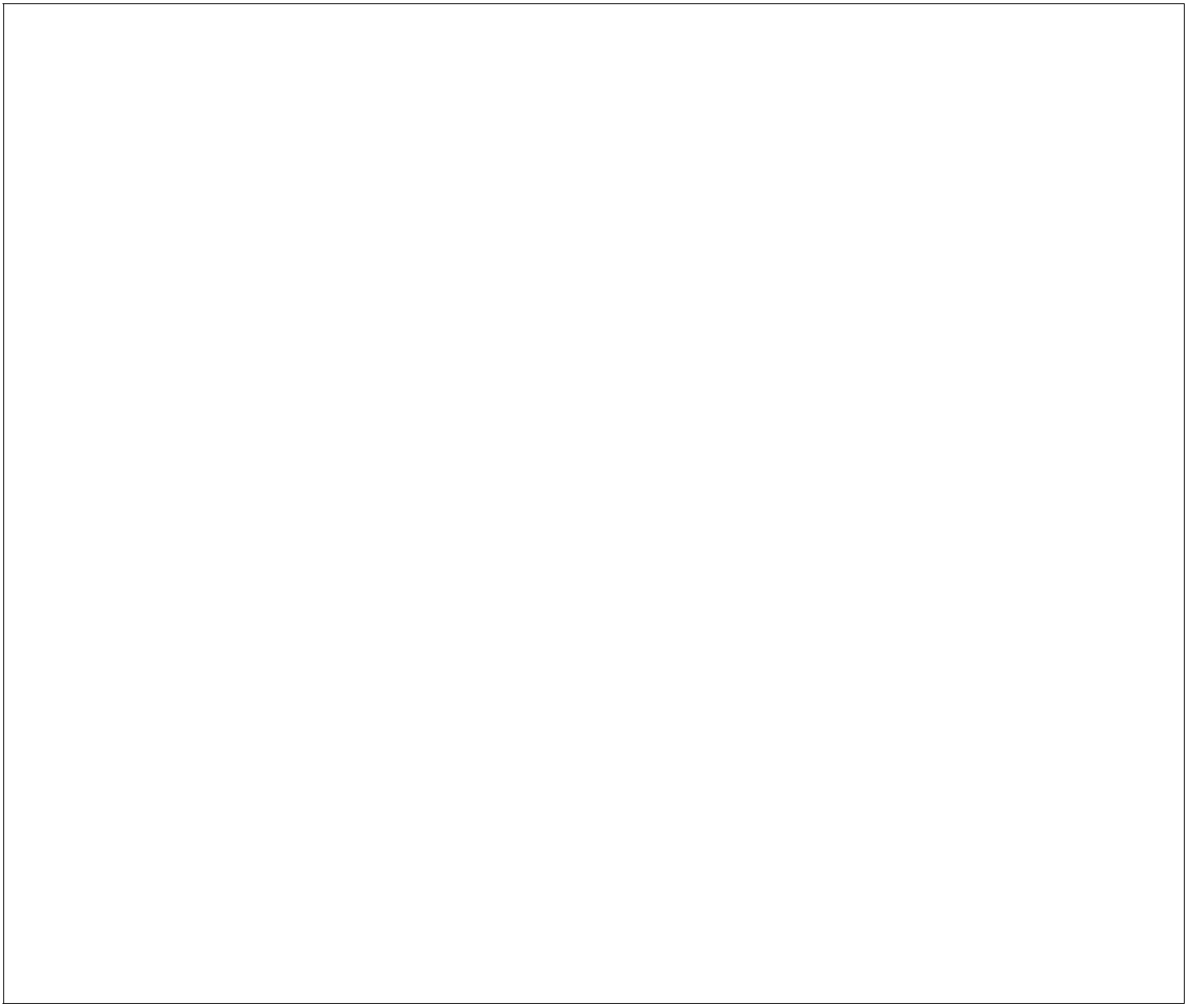

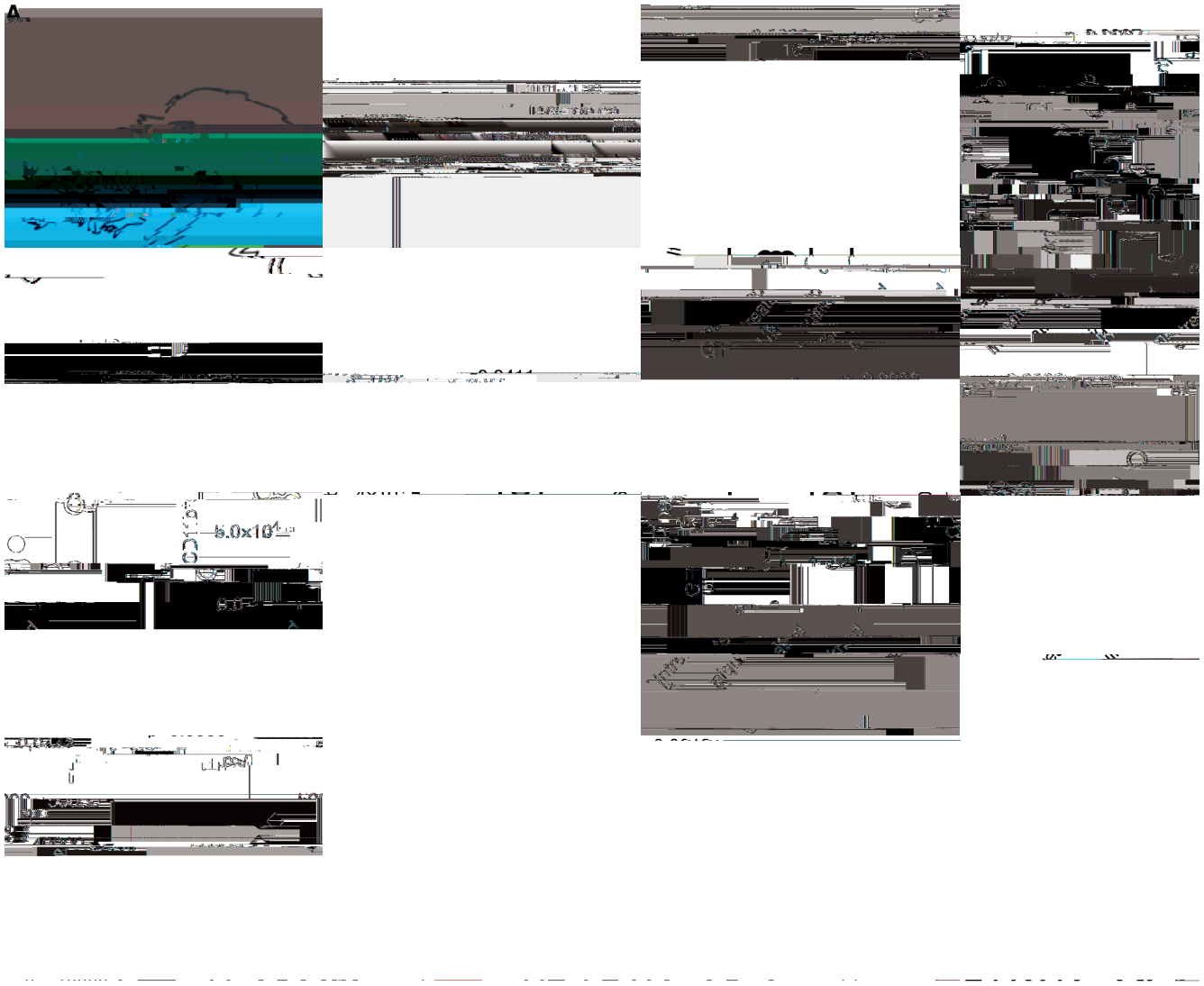

Figure 7. Imiquimod rejuvenates cDC2s in aged mice by enhancing IFN-I signalling. (**A**) Schematic representation of the experimental set-up. (**B-G**) 22–24 month-old mice were immunised subcutaneously with Eα-GFP in IFA. Half of the mice were topically treated with imiquimod cream over their immunisation sites. 22 hr after immunisation with Eα-GFP in IFA, *Ifit*◢(**B**) and *Mx*◢(**C**) mRNA expression in sorted GFP$^+$ CD11b$^+$ cDC2s was analysed by RT-qPCR. (**D-E**) Flow cytometric quantitation of total (**D**) and GFP$^+$(**E**) CD11b$^+$ cDC2 cells in the draining lymph nodes (LNs) of 22–24 month-old mice with or without imiquimod treatment. (**F-G**) Quantitation of median fluorescence intensity (MFI) levels of CD86 (**F**) and CD80 (**G**) on the surface of GFP$^+$ CD11b$^+$ cDC2s in 23-month-old mice with or without imiquimod treatment. (**H-J**) 2 month old *Ifnar*◢$^-$ and *Ifnar*◢$^{/+}$ mice were immunised subcutaneously with Eα-GFP in IFA and some of the mice were additionally treated with imiquimod cream over their immunisation sites. (**H**) 22 hr later the number of GFP$^+$ CD11b$^+$ cDC2 cells in the draining lymph nodes (LNs) were quantified. (**I-J**) Quantitation of median fluorescence intensity (MFI) levels of CD86 (**I**) and CD80 (**J**) on the surface of these GFP$^+$ CD11b$^+$ cDC2s. Bar graphs show the results of one of two independent experiments (**B-G**; n = 6 per group/experiment) or the pooled results from two experiments (**H-J**; n = 3–11 per group). Bar height corresponds to the median, and each circle represents one biological replicate. In (**B-G**)

noteworthy that both T follicular regulatory (Tfr) cells and FDCs have been linked to the age-dependent diminution of the GC response. The GC response is negatively regulated by Tfr cells (Stebegg et al., 2018), that are reported to be increased in number in aged mice and this overrepresentation of Tfr cells may result in excessive suppression of the GC response in older animals (Sage et al., 2015). There is also evidence that FDCs, stromal cells which are essential for the maintenance of the GC, are impaired in ageing (Wang et al., 2011). FDCs in aged mice form smaller networks and present fewer antigen-containing immune complexes on their surfaces after immunisation (Aydar et al., 2003; Turner and Mabbott, 2017). This is likely to affect the ability of B cells to capture antigen for presentation to Tfh cells, which in turn provide B cell growth and differentiation cues. This suggests that the age-associated defect in GC B cell expansion in mice is linked not only with a defect in T cell priming but also with other factors such as reduced antigen retention on FDCs and increased suppression by Tfr cells.

Several strategies are currently being used to enhance the response to vaccination in older persons, including modifications of adjuvants (Frech et al., 2005) or administration of increased antigen doses (Remarque et al., 1993). Hung and co-workers have shown that topical imiquimod treatment at the time of vaccination enhances the antibody responses to influenza vaccination in both younger and older persons (Hung et al., 2014; Hung et al., 2016). We have previously shown that the poor gut GC response in aged mice can be boosted by replenishing the gut microbiome with that of a younger animal (Stebegg et al., 2019). Together with the data presented here, this demonstrates that age-related defects in the GC response are not irreversible and can be targeted therapeutically to improve immune responses in older individuals. Because imiquimod can correct defective IFN-I

haemagglutinin proteins from influenza strain A/Texas/50/2012 (A/Tex12), as previously reported (Wang et al., 2015b**).**

Mouse housing and husbandry

C57BL/6, *Ifnar1*$^{-/-}$ (Skarnes et al., 2011**), *Ifnar1*$^{flox/flox}$**

Alum, or Eα-GFP in Incomplete Freund's Adjuvant (IFA). IFA (#F5506), HEL (Lysozyme from chicken egg white, #62970) and OVA (Albumin from chicken egg white; #A5503) were purchased from Sigma-Aldrich, Imject Alum (#77161) was purchased from Thermo Fisher Scientific. NP-KLH (#N-5060–25) and NP-OVA (#N-5051–100) were purchased from Biosearch Technologies. Eα-GFP fusion protein was isolated in-house from XL-1 blue *E. coli* carrying the pTRCHis-Eα-GFP vector using a protocol adapted from Rush and Brewer (2010)**. Briefly, *E. coli* carrying the pTRCHis-Eα-GFP vector were plated from glycerol stock onto LB/ampicillin agar and incubated overnight at 37 ˚C. The next day, a single colony was transferred into 5 ml LB and incubated at 37 ˚C while shaking. The next day, these 5 ml were used to inoculate 1L LB. When the culture was growing in log phase, IPTG was added to a final volume of 1 mM. The culture was left to shake overnight at 37 ˚C, then the bacteria were pelleted at 5000 g for 15 min. After discarding the supernatant, the bacterial pellet was resuspended in 20 ml lysis buffer (50 mM NaH_2PO_4, 300 mM NaCl, 10 mM Imidazole at pH 8.0) by vortexing and incubated on ice for 15 min in ice. After five repeated sonication steps on ice at 30 W for 60 s, the lysate was cleared by centrifugation at 10,000 g for 30 min. This step was repeated until all Eα-GFP was released and the bacterial pellet did not appear green anymore. The clear, green lysate was filtered first through a 0.45 μm syringe filter, then through a 0.22 μm syringe filter. Next, 200 ml of lysate were mixed with 4 ml of Ni-NTA agarose (QIAGEN #30210) and incubated at 4 ˚C. After one hour, the lysate/agarose mix was loaded onto 5 ml columns (QIAGEN #34964) and left to set. The columns were then washed twice with 25 ml of wash buffer (50 mM NaH_2PO_4, 300 mM NaCl, 20 mM Imidazole at pH 8.0). The protein was eluted by four repeated additions of 2 ml elution buffer (50 mM NaH_2PO_4, 300 mM NaCl, 250 mM Imidazole at pH 8.0) to the column. The eluate was dialysed against PBS overnight in a D-Tube Dialyzer Mega 3.5 kDa tube (Millipore # 71743–4) at 4 ˚C. On the next day, the eluate was concentrated using Centriprep centrifugal filters with an Ultracel 10K membrane (Millipore #4304) by centrifugation at 3000 g for 30 min. The concentrated protein**

were acquired on a LSRFortessa 5 and sorted with a BD FACSAria (both BD Biosciences). Flow data were analysed using FlowJo v10 software (Tree Star). The antibodies used are listed in Table 2.

To stain for pSTAT1,~2×10^6 cells isolated from the inguinal LNs of naïve mice were seeded into sterile round-bottom 96-well plates in 200 μl complete RPMI (RPMI medium (Gibco #11875093) containing 10% FBS (Sigma #F9665), 100 U/ml penicillin/streptomycin (Thermo Fisher Scientific #15140–122) and 55 μ

period, they were treated with 50 U/well recombinant murine IFNα (PBL assay science #12105–1) for 30 min and simultaneously stained with fluorochrome-coupled anti-mouse CD8a, B220 and CD11b antibodies. The cells were then washed and fixed with Cytofix (BD Biosciences #554655) for 30 min, followed by a 30 min fixation and permeabilisation step in ice-cold 90% methanol. After three washes in PBS, the cells were stained with anti-mouse pSTAT1 antibodies as well as anti-mouse CD4, CD11c, MHCII, CD172a antibodies for one hour. Samples were acquired on a LSRFortessa 5 and the flow data were analysed using FlowJo v10 software (Tree Star). The antibodies used are listed in Table 2**.**

Fluorescence-activated cell sorting (FACS)

For RT-qPCR of GFP$^+$ CD11b$^+$ cDC2, cells from total draining LNs were isolated and stained as described above. 800–4000 GFP$^+$ CD11b$^+$

RNA isolation and quantitative Real-Time PCR (RT-qPCR)

RNA isolation from ex vivo isolated cells was performed using Qiagen's RNeasy Mini or Micro Kit (#74104 and #74004) following the manufacturer's instructions. Homogenisation of the samples was achieved by vortexing for 1 min or by using QIAshredders (Qiagen #79654). RNA concentrations obtained from the RNA isolation were measured using the NanoDrop system (Thermo Fisher Scientific).

The TaqMan Gene Expression Assay (Thermo Fisher Scientific #4331182) for *Ifnb1* (Mm00439552_s1) detects genomic DNA, so RNA samples were treated with the Turbo DNA-free kit (Thermo Fisher Scientific #AM1907) according to the manufacturer's protocol to remove any contaminating genomic DNA for RT-qPCR. cDNA was generated from pre-treated RNA samples using the Quantitect reverse transcription kit (Qiagen #205311) and RT-qPCR for *Ifnb1*, *Mx1* (Mm00487796_m1) and *Ifit1* (Mm00515153_m1) was performed using the Platinum Quantitative PCR

(adjusted *p*-value cut-off p≤0.05) (Love et al., 2014**). Principal component analysis was performed using 1000 genes with the largest variances, after normalisation for batch effects with RUVSeq (**Risso et al., 2014**).**

To test for the differential expression of functionally related gene sets, a publicly available list of gene sets (Mouse_GO_AllPathways_with_GO_iea_December_24_2014_symbol.gmt.txt of Bader Lab EM_Genesets Merico et al., 2010**) was filtered for categories containing less than 20 or more than 500 genes. Resulting gene sets were tested for differential expression between young and aged samples using Seqmonk Subgroup Statistics (Kolmogorov-Smirnov test, p<0.05, average absolute z-score >1, multiple testing correction). Genes in the Responsiveness to IFN-I pathway: *Stat1, Aim2, Pyhin1, Ifi204, Ifi203, Ifi202b, Ifi205, Gbp3, Gbp2, Ifnb1, Gbp6, Htra2, Ndufa13, Trex1, Pnpt1, Tgtp1, Irf1, Igtp, Ddx41, Tmem173, Gm4951, Iigp1, Ifit3, Ifit1*.**

Publicly available datasets

PBMC RNA-Seq data from GSE45735 were used to assess an individual's IFN response over time (Henn et al., 2013**). Corresponding fastq files were obtained from SRA using the sratoolkit (https://www.ncbi.nlm.nih.gov/sra/) and aligned to GRCh38 using HISAT2 (**Kim et al., 2015**). Counting, at gene level, was performed with Rsubread (**Liao et al., 2019**). Variance stabilised normalisation (VSN, as implemented in DESeq2** Huber et al., 2002**;**

675395. We gratefully acknowledge the participation of all NIHR BioResource Centre Cambridge volunteers, and thank the NIHR BioResource Centre Cambridge and staff for their contribution. We thank the National Institute for Health Research and NHS Blood and Transplant. The views expressed are those of the authors and not necessarily those of the NHS, the NIHR or the Department of Health & Social Care.

Additional information

Funding

Funder	Grant reference number	Author
Biotechnology and Biological Sciences Research Council	BBS/E/B/000C0407	Michelle A Linterman
Biotechnology and Biological Sciences Research Council	BBS/E/B/000C0408	Michelle A Linterman
H2020 European Research Council	637801	Michelle A Linterman
H2020 Marie Skłodowska-Curie Actions	675395	Michelle A Linterman

The funders had no role in study design, data collection and interpretation, or the decision to submit the work for publication.

Author contributions

Marisa Stebegg, Data curation, Formal analysis, Investigation, Visualization, Methodology; Alexandre Bignon, Data curation, Formal analysis, Investigation, Methodology; Danika Lea Hill, Alyssa Silva-Cayetano, Edward Carr, Investigation, Visualization, Methodology; Christel Krueger, Louis Boon, Martin S Zand, James Dooley, Jonathan Clark, Investigation, Methodology; Ine Vanderleyden, Silvia Innocentin, Methodology; Jiong Wang, Investigation; Adrian Liston, Supervision, Methodology; Michelle A Linterman, Conceptualization, Data curation, Formal analysis, Supervision, Funding acquisition, Visualization, Methodology, Project administration

Author ORCIDs

Marisa Stebegg

Additional files

Supple entary files

- **Supplementary file 1. Key Resources Table.**
- **Transparent reporting form**

Data availability

Source data files are included with this manuscript. The RNA sequencing data generated for this study have been deposited at GEO (GSE133148). Further data in support of our findings are avail-

Barnett LG, Simkins HMA, Barnett BE, Korn LL, Johnson AL, Wherry EJ, Wu GF, Laufer TM. 2014. B cell antigen presentation in the initiation of follicular helper T cell and germinal center differentiation. *The Journal of Immunology* 192:3607–3617. DOI: https://doi.org/10.4049/jimmunol.1301284

Batten M, Ramamoorthi N, Kljavin NM, Ma CS, Cox JH, Dengler HS, Danilenko DM, Caplazi P, Wong M, Fulcher DA, Cook MC, King C, Tangye SG, de Sauvage FJ, Ghilardi N. 2010. IL-27 supports germinal center function by enhancing IL-21 production and the function of T follicular helper cells. *The Journal of Experimental Medicine* 207:2895–2906. DOI: https://doi.org/10.1084/jem.20100064

Baumjohann D, Preite S, Reboldi A, Ronchi F, Ansel KM, Lanzavecchia A, Sallusto F. 2013. Persistent antigen and germinal center B cells sustain T follicular helper cell responses and phenotype. *Immunity* 38:596–605. DOI: https://doi.org/10.1016/j.immuni.2012.11.020

Bentebibel S-E, Lopez S, Obermoser G, Schmitt N, Mueller C, Harrod C, Flano E, Mejias A, Albrecht RA, Blankenship D, Xu H, Pascual V, Banchereau J, Garcia-Sastre A, Palucka AK, Ramilo O, Ueno H. 2013. Induction of ICOS+CXCR3+CXCR5+ TH cells correlates with antibody responses to influenza vaccination. *Science Translational Medicine* 5:176ra32. DOI: https://doi.org/10.1126/scitranslmed.3005191

Bottrel RLA, Yang Y-L, Levy DE, Tomai M, Reis LFL. 1999. The immune response modifier imiquimod requires STAT-1 for induction of interferon, Interferon-Stimulated genes, and Interleukin-6. *Antimicrobial Agents and Chemotherapy* 43:856–861. DOI: https://doi.org/10.1128/AAC.43.4.856

Brahmakshatriya V, Kuang Y, Devarajan P, Xia J, Zhang W, Vong AM, Swain SL. 2017. IL-6 production by TLR-

Li C, To KKW, Zhang AJX, Lee ACY, Zhu H, Mak WWN, Hung IFN, Yuen K-Y. 2018. Co-stimulation with TLR7 agonist imiquimod and inactivated influenza virus particles promotes mouse B cell activation, differentiation, and accelerated antigen specific antibody production.